Proton Potential in Acetylacetone

Janez Mavri* and Jože Grdadolnik

National Institute of Chemistry, Hajdrihova 19, 1000 Ljubljana, Slovenia

Received: October 5, 2000

Proton potential in the medium-strong intramolecular hydrogen bond of acetylacetone is examined on various ab initio and DFT levels. Semiempirical MO methods AM1 and PM3 turn out to be inadequate for the present system. It was shown that the proton donor−proton acceptor distance influences the barrier height while both CO distances introduce the asymmetry to the otherwise symmetric proton potential Ab initio data are fitted to a computationally inexpensive two-state empirical valence bond potential suitable for molecular simulations.

1. Introduction

The relevance of strong hydrogen bonding in enzymatic catalysis is an ongoing subject of discussion.[1−3] Pentane-2,4-dione also known as acetylacetone (ACAC) can exist in two tautomeric forms: keto and enol. The latter form is characterized by an intramolecular hydrogen bond. The keto/enol equilibrium spurred much research. It has been demonstrated that the tautomeric equilibrium depends on both temperature and solvent.[4]

The structure of the enol tautomer of ACAC is shown in Figure 1. The enol content varies from 13% in aqueous solution to 98% in cyclohexane.[4] The percentage of the enol form correlates with the dielectric constant of solvent. Buemi and Gandolfo[5] have demonstrated using MO calculations that the keto tautomer of ACAC has a lower dipole moment than the enol. Therefore, one can conclude that specific interactions with solvent molecules, such as hydrogen bonds, play the dominant role in this tautomeric equilibrium. The keto−enol equilibrium can be shifted significantly if one replaces the methyl groups with other substituents.

The structure of ACAC is available from gas-phase electron-diffraction experiments.[6] The measured proton donor−proton acceptor distance is 2.512 Å. The X-ray structure of ACAC was obtained when ACAC turned up as a solvate in a drug complex.[7]

The crystal structure reveals an OO distance of 2.535 Å. Infrared spectra of acetylacetone reveal that an asymmetric OH stretching band occurs at 2750 cm^{-1}, which then drops to 1950 cm^{-1} with deuteration.[8,9] Experimental spectra correspond to ACAC in dichloromethane solution. According to the classification of Hibbert and Emsley[4] such spectra are associated with medium strong hydrogen bonds.

Replacement of the methyl groups of ACAC with hydrogen atoms gives rise to malonaldehyde. The simpler analogue, malonaldehyde, has been the subject of numerous experimental[10−12] and theoretical[13] studies. The equilibrium of malonaldehyde in polar solvents is strongly shifted toward the keto tautomer, which has no intramolecular hydrogen bond. Since the main purpose of our work is a comparison of the simulated proton dynamics of a strong intramolecular hydrogen bond (using the available experimental data) in polar solution, we have chosen to consider ACAC rather than malonaldehyde in this study. Recently ACAC has been the subject of ab initio studies,[14] path-integral molecular dynamics simulations,[15] time-dependent self-consistent field quantum-classical MD, and adiabatic quantum-classical MD.[16]

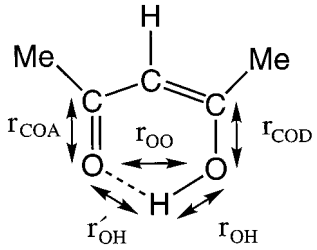

Figure 1. Structure of the enol tautomer of acetylacetone.

In this article we perform ab initio, DFT and semiempirical MO calculations of the structure and proton potential in acetylacetone. The main aim of this work is to construct an empirical, computationally inexpensive generator of the proton potential in ACAC. Since the empirical proton-potential function will be applied in the quantum-dynamical study of ACAC, one should keep the computational costs low. In this article only the CO−H−OC moiety is considered. The proton potential, thus, explicitly depends on the OO distance and both CO distances. One should bear in mind that variation of the OO distance is inherent in more than one normal vibrational mode that includes CCC and OCC bendings and dihedral angle changes. We are aware that the proton potential is influenced by all other degrees of freedom in ACAC, but the available computer power did not allow for inclusion of more degrees of freedom. The residual intramolecular degrees of freedom in our model do not, therefore, have a direct influence on the proton potential. They are treated on the molecular mechanics level using standard GROMOS force field parameters,[17] which will be described in our article dealing with quantum dynamical simulation proton transfer in ACAC.[18] The proton potential function is required in the numerical integrations that give rise to several matrix elements at every classical time step. We followed the strategy of Warshel and co-workers[19] and developed the proton potential using the functional form of the empirical valence bond (EVB) function.

The organization of this article is as follows: section 2 describes the performed ab initio and DFT calculations, section

* To whom correspondence should be addressed. E-mail: janez@kihp2.ki.si.

10.1021/jp003667g CCC: $20.00
Published on Web 02/13/2001

TABLE 1: Classical Energy Barriers for the Proton Transfer in Acetylacetone Calculated on Various Levels of Theory[a]

level of theory	$\Delta E^{\#}$	OO_{asym}	OH_{asym}	COD_{asym}	COA_{asym}	OO_{sym}	CO_{sym}
AM1	20.72	2.822	0.975	1.360	1.245	2.353	1.302
PM3	24.44	2.636	0.967	1.347	1.233	2.266	1.289
HF/3-21G(d)	6.198	2.563	0.986	1.340	1.238	2.341	1.286
HF/4-31G(d)	9.399	2.624	0.964	1.314	1.212	2.331	1.259
HF/6-31G(d,p)	8.214	2.620	0.960	1.314	1.215	2.321	1.261
HF/6-31+G(d,p)	8.191	2.624	0.960	1.315	1.216	2.321	1.262
HF/6-311+G(2d,2p)	8.293	2.620	0.956	1.312	1.209	2.319	1.257
MP2/3-21G	5.644	2.575	1.027	1.368	1.282	2.414	1.321
MP2/4-31G(d)	3.773	2.577	1.008	1.333	1.252	2.383	1.289
MP2/6-31G(d,p)	7.054	2.546	1.002	1.333	1.256	2.362	1.291
MP2/6-31+G(d+p)	2.503	2.547	1.005	1.336	1.260	2.365	1.295
MP2/6-311+G(2d,2p)	2.669	2.509	1.007	1.320	1.257	2.363	1.287
B3LYP/3-21G	0.43	2.457	1.083	1.337	1.284	2.398	1.311
B3LYP/6-31G(d,p)	1.66	2.507	1.018	1.322	1.254	2.367	1.287
B3LYP/6-31+G(d,p)	1.74	2.514	1.016	1.325	1.256	2.367	1.290
B3LYP/6-311+G(2d,2p)	2.12	2.522	1.009	1.322	1.248	2.368	1.284

[a] The barriers $\Delta E^{\#}$ are given in kcal mol^{-1}. All the distances are given in Å. OO_{asym} and OH_{asym} are the OO and OH distances of the fully optimized structure. COD_{asym} and COA_{asym} are the CO distances of the proton donor and the proton acceptor of the fully optimized structure. OO_{sym} and CO_{sym} are the OO and CO distances of the structure in the transition state.

3 describes the fitting of the DFT proton potential to the EVB form, and section 4 gives concluding remarks.

2. Ab Initio, DFT, and Semiempirical MO Calculations

The calculated proton potential in hydrogen bonded systems is very sensitive to the applied level of theory. There is a general rule that one should use large, flexible basis sets containing a significant number of polarization functions. Proper inclusion of the electron correlation is mandatory if one wants to reproduce the barrier for the proton transfer.[20] Typically, the barrier increases with the size of the basis set and decreases with the inclusion of the electron correlation. The electron correlation was taken into account by performing MP2 calculations (Moller−Plesset perturbation of the second order). MP2 calculations include a significant part of the correlation energy. A computationally less demanding alternative to the MP2 calculations is the application of density functional (DFT) methods. The DFT method that includes the correlation functional proposed by Becke[21] and the correlation functional proposed by Lee, Yang, and Parr is B3LYP. We applied this method as implemented in the Gaussian-94[22] program package. Different investigators have demonstrated that the B3LYP functional is the best DFT functional currently available to describe the proton potential in hydrogen bonded systems.[23−26]

The classical barrier to intramolecular proton tranfer in ACAC was calculated in order to critically examine various quantum-chemical methods. The semiempirical methods AM1 and PM3 were also considered since they are very promising for use in the mixed quantum-classical calculations where a huge number of energies and forces should be evaluated. The barrier was estimated to be the energy of the structure with the constraint of equal proton−proton donor and proton−proton acceptor distances minus the energy of the fully geometrically optimized molecule. The fully optimized structure corresponds to reactants and the products, while the structure optimized with the constraint of equal OH distances corresponds to the transition state. The activation energy calculated in this manner corresponds to the classical barrier, so quantal effects, such as zero point energy, are not taken into account. The barrier heights calculated on various levels of theory are shown in Table 1.

In the present case, it turns out that semiempirical methods PM3 and AM1 fail to predict either the energy or the metric parameters relevant for the proton transfer. The calculated OO distances are too long and the calculated barriers have the values of 24.44 and 20.72 kcal mol^{-1} on the PM3 and AM1 levels, respectively.

Ab initio calculations on the Hartree−Fock (HF) level yield particularly high barriers. The barriers increase almost monotonically from 6.20 kcal mol^{-1} on the 3-21G level to 8.29 kcal mol^{-1} on the 6-311+G(2d,2p) level. The latter basis set is triple-ζ and is augmented with a double set of polarization functions on heavy and light atoms. Moreover, the diffuse functions are placed on all of the heavy atoms, to improve the calculated proton−donor and proton−acceptor properties of the oxygen atoms involved in hydrogen bonding. On the Hartree−Fock level the basis set 4-31G(d) gives rise to an especially high barrier of 9.40 kcal mol^{-1}; the predicted OO distance was 2.624 Å. The barrier seems to be too high and the calculated OO distance is roughly 0.1 Å longer than the experimental value. This level of theory was used by Hinsen and Roux for exploration of the Born−Oppenheimer hypersurface for the proton transfer in ACAC.[14]

MP2 calculations give rise to decreased barriers, which are associated with OO distances shorter than those predicted by the HF calculations. It is worthwhile to emphasize the dramatic effect of adding diffuse functions to the calculated barrier. When the basis set 6-31G(d,p) is augmented with diffuse functions on the heavy atoms, the barrier on the MP2 level drops from 7.05 to 2.50 kcal mol^{-1}. Interestingly, the OO distance for the fully optimized forms is practically the same for both cases. Comparison of the absolute energies on the HF level using different basis set reveals that, by using the basis set 6-31+G-(d,p), we are still far away from the Hartree−Fock limit.

B3LYP calculations predict even lower barriers than the MP2 calculations. The barrier slightly increases with the size of the basis set. The largest basis set we considered here is 6-311+G-(2d,2p). This basis set combined with the B3LYP calculation should, according to our experience, provide a faithful enough description of the hypersurface to allow it to be used in the quantum-dynamical calculations and calculations of vibrational spectra associated with the proton transfer. Evaluation of the single point energy and forces using this level of theory takes about 6 h of CPU on a Hewlett-Packard C180 workstation. Bearing in mind that the MP2 calculations include only part of the correlation energy, one should expect that application of a higher level of theory (MP4 or Configuration Interaction) would further decrease the barrier. The choice of the B3LYP 6-311+G-(2d,2p) levels seems to be justified, since it would not be

possible to perform the calculations on a higher level with the available computer power.

Table 1 reveals the general trend that longer OO distances yield higher barriers. Therewith is associated considerable shrinking of the OO distance associated with driving the system from the minimum to the transition state. Shortening of the OO distance is more pronounced with methods that give rise to a higher proton tranfer barrier. On the other hand, all of the applied methods, including semiempirical MO methods, reproduce quite nicely the variations in CO distances corresponding to the proton donor and the proton acceptor during the proton transfer.

The main goal of this work was to construct a computationally tractable empirical expression for the proton potential as a function of the OO distance and both CO distances on the basis of ab initio calculated points. Therefore, we believe that the applied level B3LYP/6-311+G(2d,2p) is a good compromise between the reliability of the results and the spent CPU time.

3. Empirical Valence Bond Form

The B3LYP/6-311+G(2d,2p) level of theory was used to fit the intramolecular proton potential and the charges that reproduce the electrostatic potential in the vicinity of the ACAC molecule. The proton potential was calculated for different combinations of CO and OO distances. We considered three values for the OO distance and three values for the CO distance. For a given OH distance all other degrees of freedom but the OO and both CO distances were optimized. For description of the intramolecular degrees of freedom in ACAC one would need 39-dimensional hypersurface, which is impossible to construct because of high computational costs. The aim of this work is to fit the proton potential depending on the OO and the two CO distances. The hypersurface is thus four-dimensional, meaning that a significant number of DFT calculated points are required.

We determined proton potentials using several combinations of CO and OO distances. The global B3LYP/6-311+G(2d,2p) minimum is associated with an OO distance of 2.523 Å and CO distances of 1.322 and 1.248 Å for the proton donor and the proton acceptor, respectively. The structure optimized under the constraint of equal OH distances results in equal CO distances of 1.284 Å. We also took into consideration the variations in OO distance, so that the resulting energy increase did not exceed a few kcal mol^{-1}, i.e., the value still thermally accessible in molecular simulations. Therefore, in addition to the equilibrium OO distance of 2.523 Å, the distances 2.362 and 2.600 Å were also considered. Calculations of the proton potentials as a function of the OO and CO distances are a four-dimensional problem. Variation of the proton potential with other intramolecular degrees of freedom (like CC distances) would be desirable, but the available CPU power does not allow for such scans.

The only reason for fitting the intramolecular proton potential to the relatively simple functional form is that this allows a computationally inexpensive evaluation of the potential energy and other derivatives. Initially, we applied four-dimensional spline interpolation. This attempt failed, due to artifacts of the spline behavior at the boundary and to the relatively low number of points used in the interpolation. The empirical valence bond (EVB) method is an attractive method for making an approximate description of the Born−Oppenheimer surfaces. This method, pioneered by Warshel, has found wide application in the study of chemical reactions in solutions and enzymatic environments. For an excellent review of the EVB methodology, see ref 19.

In this article we describe the proton potential in ACAC using two valence bond structures. In one valence bond structure the proton is attached to the proton donor and in the other to the proton acceptor. The effects in variations of the OO and CO distances were also considered. During the fitting procedure we tried to reproduce the positions and energies of the minima and barrier heights. The OH bonds were described by two Morse functions as follows

$$U_1 = D(\exp(-2b(r_{OH} - R_0)) - 2\exp(-b(r_{OH} - R_0))) + f_{asym}(r_{COD} - R_{CO}) \quad (1)$$

and

$$U_2 = D(\exp(-2b(r'_{OH} - R_0)) - 2\exp(-b(r'_{OH} - R_0))) + f_{asym}(r_{COA} - R_{CO}) \quad (2)$$

where r_{OH} refers to the proton−proton donor distance and r'_{OH} to the proton−proton acceptor distance. r_{COD} is the CO distance at the proton donor site and r_{COA} is the CO distance at the proton acceptor site. r'_{OH} is calculated as $r'_{OH} = s + r_{OO} - r_{OH}$, where r_{OO} is the OO distance and the shift s of 0.1 Å reflects the curvilinear path of the proton's motion. R_0 is the unperturbed OH bond length, D is the classical dissociation energy of the isolated OH bond, and parameter b is related to the second derivative of the Morse function at the minimum energy. The last terms in the previous two equations describe the asymmetry of the proton potential due to variation of the CO bond lengths of the proton donor and the proton acceptor. The CO distance corresponding to the proton donor is longer than the CO distance corresponding to the proton acceptor. R_{CO} is the CO bond length of the structure optimized under the constraint of equal OH distances.

The two EVB structures give rise to the bonding hypersurface E'

$$E' = \frac{U_1 + U_2}{2} - \sqrt{\left(\left(\frac{U_1 + U_2}{2}\right)^2 - U_1U_2 + \epsilon^2\right)} \quad (3)$$

where ϵ is the coupling term. The complete hypersurface $E = E(r_{OH},r_{OO},r_{COD},r_{COA})$ for the CO..H..OC moiety of ACAC was obtained by adding additional terms to the E' corresponding to changes in both CO bond lengths and OO bond lengths from their equilibrium position

$$E = E' + E_{COD} + E_{COA} + E_{OO} + S \quad (4)$$

The additional terms were necessary since the two Morse functions giving rise to the two EVB structures were not able to describe the energetics of the CO..H..OC moiety properly. The terms in the equation above read as follows:

$$E_{COD} = \frac{1}{2}f_{CO}(r_{COD} - R_{CO} + A)^2 \quad (5)$$

$$E_{COA} = \frac{1}{2}f_{CO}(r_{COA} - R_{CO} + A)^2 \quad (6)$$

$$E_{OO} = \frac{1}{2}f_{OO}(r_{OO} - B)^2 \quad (7)$$

The term S is a constant which was chosen so that the minimum energy equals zero. The harmonic terms for the OO and the CO distances can be understood as a correction to the Morse functions to improve the quality of the fit. The shortening of the equilibrium CO distances for $A = 0.09$ Å significantly

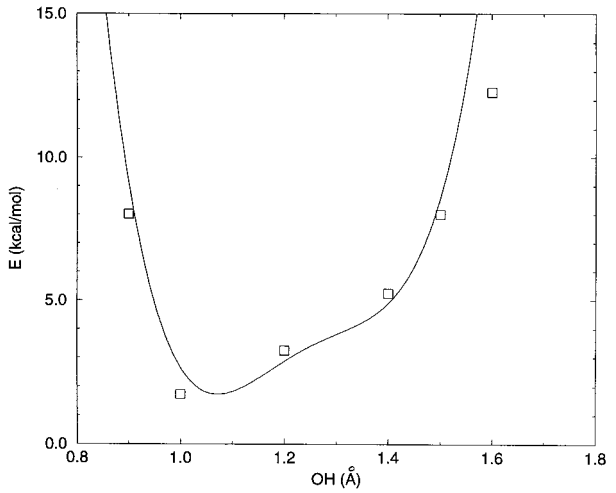

Figure 2. B3LYP/6-311+G(2d,2p) calculated proton potential for an OO distance of 2.362 Å, proton donor CO distance of 1.322 Å, and proton acceptor CO distance of 1.248 Å. Squares represent the DFT calculated points. All other degrees of freedom were optimized at each point. The line is the EVB approximated potential.

TABLE 2: Parameters Used in the Empirical Valence Bond Description of Acetylacetone. Equations 1−7. All Quantities Are in Units Derived from Distances in Å and Energies in Kcal Mol^{-1}

parameter	value
D	284 kcal mol^{-1}
R_0	0.952
b	1.49 Å^{-1}
ϵ	115 kcal mol^{-1}
f_{asym}	167 kcal mol^{-1}Å^{-1}
f_{CO}	1134 kcal mol^{-1}Å^{-2}
R_{CO}	1.284 Å
f_{OO}	229.24 kcal mol^{-1}Å^{-2}
A	0.09 Å
B	2.7648 Å
S	340.35 kcal mol^{-1}

improved the quality of the fit. The additional harmonic term for the OO distance involves the equilibrium OO distance $B =$ 2.7648 Å. This value is roughly 0.23 Å longer than the DFT calculated OO equilibrium value, but it significantly improves the quality of the fit. The parameters used in the equations above are a result of the fitting to the B3LYP/6-311+G(2d,2p) level calculations and are collected in Table 2. The EVB proton potentials and corresponding DFT calculated proton potentials are shown in Figures 2−7. The agreement is not perfect, but the EVB form at least semiquantitatively reproduces the barriers, positions, and minima for a wide range of OO and CO distances. An exception is the proton potential for the OO distance of 2.60 Å (Figure 7) where the barrier is underestimated. Fortunately this structure is energetically unfavorable and it does not contribute much to the calculated spectrum.

The classical barrier for the proton transfer depends on the OO distance: for increased OO distances the barrier is increased, for decreased OO distance the barrier is lowered, and for extremely short OO distances it even disappears.

Variation in CO bond lengths introduces asymmetry to the proton potential. The CO bond length of the proton donor is elongated relative to the CO bond length of the proton acceptor. The main aim of this work is to construct a computationally inexpensive force field for ACAC, which is suitable for quantum-dynamical simulations. We describe only the CO−H−OC moiety of ACAC using EVB, while all other degrees of freedom are described by molecular mechanics using the GROMOS force field.[17]

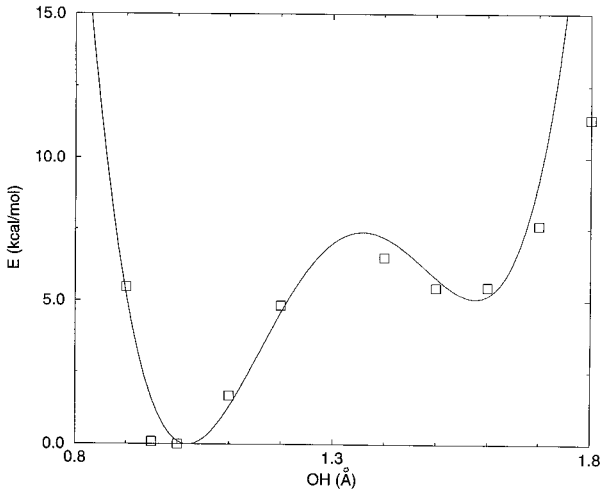

Figure 3. B3LYP/6-311+G(2d,2p) calculated proton potential for an OO distance of 2.523 Å, proton donor CO distance of 1.322 Å, and proton acceptor CO distance of 1.248 Å. The lowest point of this proton potential is the global minimum of the system.

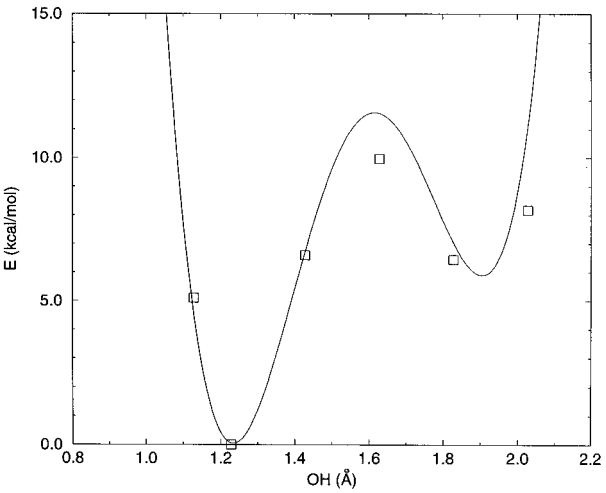

Figure 4. B3LYP/6-311+G(2d,2p) calculated proton potential for an OO distance of 2.600 Å, proton donor CO distance of 1.322 Å, and proton acceptor CO distance of 1.248 Å.

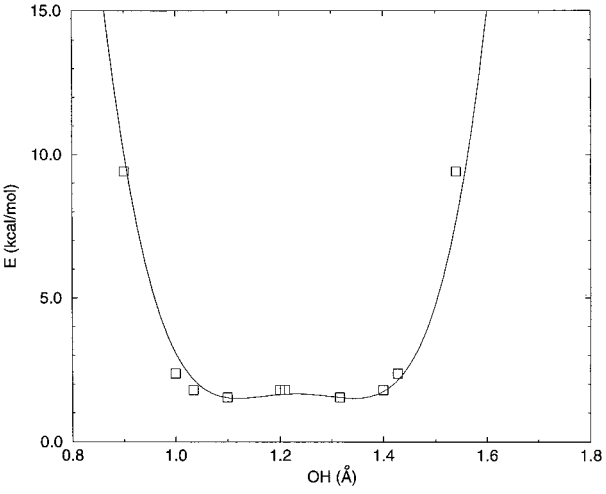

Figure 5. B3LYP/6-311+G(2d,2p) calculated proton potential for an OO distance of 2.362 Å, proton donor CO distance of 1.284 Å, and proton acceptor CO distance of 1.284 Å.

Vibrational analysis of the fully minimized ACAC was performed on the B3LYP/6-311+G(2d,2p) level in the harmonic approximation. Assignment of the vibrational modes was

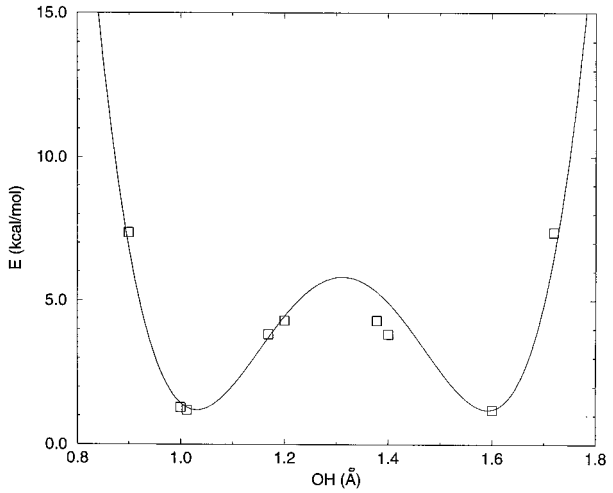

Figure 6. B3LYP/6-311+G(2d,2p) calculated proton potential for an OO distance of 2.523 Å, proton donor CO distance of 1.284 Å, and proton acceptor CO distance of 1.284 Å.

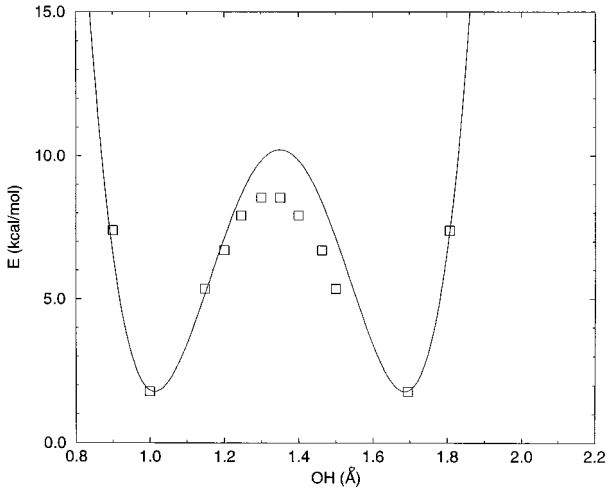

Figure 7. B3LYP/6-311+G(2d,2p) calculated proton potential for an OO distance of 2.600 Å, proton donor CO distance of 1.284 Å, and proton acceptor CO distance of 1.284 Å.

performed by visualization of the eigenvectors. Asymmetric OH stretching was calculated to be 2953 cm^{-1}. Out-of-plane OH bending was coupled with the C−C−C out-of-plane deformations and was associated with 1642 cm^{-1}. The OO stretching was also coupled with the C−C−C skeleton bending and had a frequency of 396 cm^{-1}. Variation of the OO distance is inherent to more than one vibrational mode. In this work, we have considered variation of the OO distance to be a special mode in order to keep the number of relevant degrees of freedom for proton potential as low as possible. All other intramolecular degrees of freedom in ACAC, except the CO−H..OC moiety, have been described using the molecular mechanical description with a GROMOS force field and will be detailed in a future article dealing with the quantum-classical dynamics of ACAC. We expect to see coupling of the OH motion with the skeleton modes, in particular with the CC stretchings.

To simulate ACAC in chloroform solution, one needs to know certain nonbonding parameters, particularly atomic charges. The atomic charges were calculated for various OH distances according to the procedure that fits the atomic charges so that they reproduce the electrostatic potential in the vicinity of the molecule.[27] Calculations on the B3LYP/6-311+G(2d,2p) level included the solvent reaction field according to the method of Miertuš et al.[28] The calculated charges correspond to the polarized values and will be reported on a future article describing the quantum dynamical simulation of ACAC.

4. Conclusions

The proton potential in acetylacetone was examined by semiempirical MO methods, ab initio methods on the HF and MP2 levels, and by the DFT method using the exchange functional proposed by Becke and the correlation functional of Lee, Yang, and Parr. The semiempirical method yields an unreasonably high barrier to the proton transfer. The Hartree−Fock calculations also yield a too high barrier. The MP2 and B3LYP applied with large, flexible basis sets yield a classical barrier of under 3.0 kcal mol^{-1}. The part of the hypersurface relevant for the proton tranfer was explored with the B3LYP/6-311+G(2d,2p) method, yielding a classical barrier of 2.12 kcal mol^{-1}. Variations in the proton potential with respect to the OO distance and both CO distances were considered. The former influences the barrier height, while the latter introduce asymmetry. The potential was fitted to the two-state empirical valence form suitable for quantum-dynamical molecular simulations.

Note Added in Proof. When the manuscript was in preparation a crystal structure of acetylacetone was reported (Boese, R.; Antipin, M. Yu.; Bläser, D.; Lyssenko, K. A. *J. Phys. Chem. B* **1998**, *102*, 8654−8660).

Acknowledgment. The authors are grateful to Prof. Benoit Roux, University of Montreal, Prof. Dušan Hadži, National Institute of Chemistry and Dr. Adam Fedorowiz, University of Wroclaw, for many stimulating discussions and a critical reading of the manuscript, and Ms. Charlotte Taft for linguistic corrections. We are grateful to the referee for many useful comments and suggestions. This work was supported by a grant from the Slovenian Ministry of Science and Technology.

References and Notes

(1) Cleland, W. W.; Kreevoy, M. M. *Science* **1994**, *264*, 1887−1890.
(2) Warshel, A.; Papazyan, A.; Kollman, P. A. *Science* **1994**, *269*, 102−104.
(3) Cleland, W. W.; Kreevoy, M. M. *Science* **1995**, *269*, 104.
(4) Hibbert, F.; Emsley, J. Chapter *Hydrogen Bonding and Chemical Reactivity*; Academic Press: Amsterdam, 1990; Vol. 26, pp 256−379.
(5) Buemi, G.; Gandolfo, C. *J. Chem. Soc., Faraday Trans.* **1989**, *85*, 215.
(6) Iijima, K.; Ohnogi, A.; Shibata, S. *J. Mol. Struct.* **1987**, *156*, 111.
(7) Camerman, A.; Mastropaolo, D.; Camerman, N. *J. Am Chem. Soc.* **1983**, *105*, 1584.
(8) Bratoz, S.; Hadzi, D.; Rossmy, G. *Trans. Faraday Soc.* **1956**, *52*, 1956.
(9) Ernstbrunner, E. E. *J. Chem. Soc. A* **1970**, p 1558.
(10) Baughcum, S. L.; Duerst, R. W.; Rowe, W. F.; Smith, Z.; Wilson, E. B. *J. Am. Chem. Soc.* **1981**, *103*, 6296−6303.
(11) Baughcum, S. L.; Smith, Z.; Wilson, E. B.; Duerst, R. W. *J. Am. Chem. Soc.* **1984**, *106*, 2260−2265.
(12) Turner, P.; Baughcum, S. L.; Coy, S.; Smith, Z. *J. Am. Chem. Soc.* **1984**, *106*, 2265−2267.
(13) Wolf, K.; Mikenda, W.; Nusterer, E.; Schwartz, K. *J. Mol. Struct.* **1997**, *448*, 201−207.
(14) Hinsen, K.; Roux, B. *J. Comp. Chem.* **1997**, *18*, 368−380.
(15) Hinsen, K.; Roux, B. *J. Chem. Phys.* **1997**, *106*, 3567−3577.
(16) Sahrafeddin, O. A.; Hinsen, K.; Carrington, T.; Roux, B. *J. Comput. Chem.* **1997**, *18*, 1760−772.
(17) van Gunsteren, W. F.; Berendsen, H. J. C. *GROMOS-87 manual*; Biomos, B. V., Ed.; Groningen: The Netherlands, 1987; Nijenborgh 4, 9747 AG.
(18) Mavri, J.; Grdadolnik, J. *J. Phys. Chem. A* **2001**, *105*, 2045.
(19) Warshel, A. *Computer Modeling of Chemical Reactions in Enzymes and Solutions*; John Wiley and Sons: New York, 1991.
(20) Scheiner, S.; Szczesniak, M. M.; Bigham, L. D. *Int. J. Quantum Chem.* **1983**, *23*, 739−751.
(21) Becke, A. D. *J. Chem. Phys.* **1993**, *98*, 5648−5652.

(22) Frisch, M. J.; Trucks, G. W.; Schlegel, H. B.; Gill, P. M. W.; Johnson, B. G.; Robb, M. A.; Cheeseman, J. R.; Keith, T.; Petersson, G. A.; Montgomery, J. A.; Raghavachari, K.; Al-Laham, M. A.; Zakrzewski, V. G.; Ortiz, J. V.; Foresman, J. B.; Peng, C. Y.; Ayala, P. Y.; Chen, W.; Wong, M. W.; Andres, J. L.; Replogle, E. S.; Gomperts, R.; Martin, R. L.; Fox, D. J.; Binkley, J. S.; Defrees, D. J.; Baker, J.; Stewart, J. P.; Head-Gordon, M.; Gonzalez, C.; Pople, J. A. *Gaussian 94*, revision B.3; Gaussian, Inc.: Pittsburgh, PA, 1995.

(23) Novoa, J. J.; Sosa, C. *J. Phys. Chem.* **1995**, *99*, 15837.

(24) Barone, V.; Adamo, C. *Chem. Phys.* **1996**, *105*, 11007.

(25) Pudzianowski, A. *J. Phys. Chem.* **1996**, *100*, 4781.

(26) Fores, M.; Duran, M.; Sola, M.; Adamowicz, L. *J. Comput. Chem.* **2000**, *21*, 257−269.

(27) Besler, B. H.; Merz, K. M., Jr.; Kollman, P. A. *J. Comput. Chem.* **1990**, *11*, 431.

(28) Miertus, S.; Scrocco, E.; Tomasi, J. *Chem. Phys.* **1981**, *55*, 117.